

Kinetic electron emission from the selvage of a free-electron-gas metal

S. Lederer, K. Maass, D. Blauth, and H. Winter*

Institut für Physik, Humboldt Universität zu Berlin, Invalidenstrasse 110, D-10115 Berlin, Germany

HP. Winter and F. Aumayr

Institut für Allgemeine Physik, Technische Universität Wien, Wiedner Hauptstrasse 8-10, A-1040 Vienna, Austria

(Received 18 December 2002; published 17 March 2003)

Coincident measurements of projectile energy loss and kinetic electron emission yield for grazing scattering of 150 eV/amu to some keV/amu neutral hydrogen and helium atoms from an atomically clean and flat Al(111) surface allow us to correlate electron emission and inelastic interaction mechanisms at a metal surface. Our data show evidence for a threshold behavior of kinetic electron emission which is interpreted by energy transfer in binary encounters of projectiles in the electron selvage of a quasi-free electron gas. Contributions of electron emission to projectile energy loss are found to be negligibly small.

DOI: 10.1103/PhysRevB.67.121405

PACS number(s): 79.20.Rf, 61.85.+p, 79.60.Bm

Ionization of atoms, molecules, and complex matter by impact of particles (electrons, atoms, and ions) is of fundamental interest and relevant for many practical applications. Since first treatments of electron-impact ionization of atoms by Thomson,¹ numerous authors have considered the ionization process in a basically classical way, e.g., Thomas,² Gryzinsky,³ or Kingston.⁴ This led to semiempirical ionization formulas used in atomic and plasma physics.^{5,6}

For ionization of solids, one distinguishes between two mechanisms (1) *kinetic electron emission* (KE) mediated by the kinetic energy of the projectile and (2) *potential electron emission* (PE) induced by the internal energy of excited or ionized projectiles.^{7,8} In reference to gas-phase collisions mentioned above, it is tempting to ask to what extent the KE process may be described by classical concepts, apart from the KE threshold that corresponds to the minimum-energy transfer of projectiles to electrons in a solid to reach vacuum. Such a classical treatment is probably most appropriate for metals that can be described as a free-electron system (jellium).⁹ Here the threshold of projectile velocity v_{th} for KE is derived by assuming maximum-energy transfer of atomic projectiles to free electrons of the metal with Fermi energy E_F (velocity v_F) in order to overcome the surface work function W ⁸

$$v_{th} = \frac{v_F}{2} [(1 + W/E_F)^{1/2} - 1]. \quad (1)$$

Experimental studies on the threshold behavior of KE for impact of light ions were not conclusive with respect to v_{th} so far.⁸ Aside from uncertainties inherent in the separation of contributions from PE to electron yields by using ionized projectiles, KE may be caused by several other mechanisms,^{8,10} in particular, for heavier atomic projectiles by electron promotion in close collisions with target atom cores.¹¹ A specific technical problem for a reliable determination of v_{th} concerns small electron yields as low as $\gamma \leq 10^{-3}$ electrons/projectile which are extremely difficult to obtain from measurements of ion and electron currents.¹² Furthermore, KE induced by impact of atomic projectiles is

accompanied by (electronic) excitation of the target which cannot be elucidated by KE measurements only.

In this paper, we report on studies on the threshold behavior of KE for grazing incidence scattering of fast neutral hydrogen and helium atoms from an Al(111) surface. For this specific collision geometry, scattering of projectiles proceeds in the regime of planar surface channeling¹³⁻¹⁵ with well-defined trajectories and in terms of specular reflection at a distance of some a.u. (atomic units) in front of the topmost layer of surface atoms. Projectiles interact with electrons in the selvage of the surface only and their energy loss can be used to monitor the total inelastic interaction processes. Thus, KE will be studied here by the detection of emitted electrons in coincidence with scattered projectiles and their energy loss. This allows us to correlate electron emission from and inelastic processes in the selvage of a free-electron metal in order to gain deeper insights into the microscopic interaction mechanism. The technique was successfully applied in studies of scattering of atoms and ions from surfaces of ionic crystals with wide-band gaps, where the formation of negative ions was revealed as common precursor for electron emission and excitations of valence-band electrons located at halogen sites (surface excitons).^{16,17}

In our experiments, neutral H⁰ and He⁰ projectiles with energies ranging from 150 eV/amu to some keV/amu are scattered from a well prepared atomically clean and flat Al(111) surface under a grazing angle of incidence $0.5^\circ \leq \Phi_{in} \leq 2^\circ$. Time-of-flight (TOF) spectra for projectiles reflected from the surface are recorded in coincidence with electron multiplicities for each scattering event by means of an electron number detector [surface-barrier detector (SBD) biased to +25 kV, detector pulse heights proportional to electron number ejected per projectile impact on surface^{12,18}]. Chopped beams of fast H⁰ and He⁰ atoms (neutralized in gas target) hit the sample under high index (random) azimuthal orientation, and specularly reflected projectiles are recorded 1.38 m behind the target by means of a channel-plate electron multiplier. Electrons emitted from the Al surface are collected by a weak electric field owing to a bias of some 10 V applied to a highly transparent grid about 1 cm in front of the target. The target surface is kept at a base

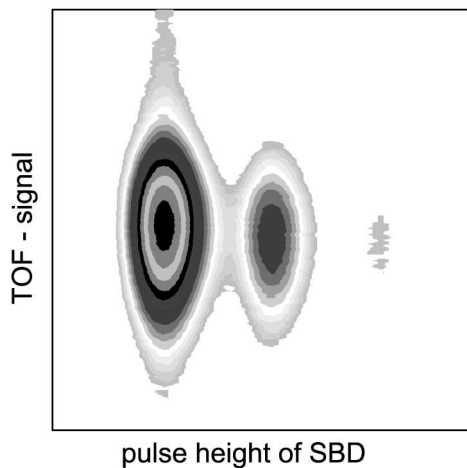


FIG. 1. Contour plot of TOF signal vs SBD pulse height for 1.5 keV H^+ atoms scattered from Al(111) with $\Phi_{in} = 1.88^\circ$.

pressure of some 10^{-11} mbar and at room temperature. As detailed in a recent paper,¹⁹ the coincident detection of projectile energy loss with number of emitted electrons is achieved by relating the TOF signals to the pulse heights of the SBD. Since the efficiency for detection of electrons by our setup is close to 1, corrections on electron number spectra can be neglected here.

As an example of coincident TOF and electron number spectra, we show in Fig. 1 a two-dimensional contour plot for scattering of 1.5 keV H^+ atoms from Al(111) under $\Phi_{in} = 1.88^\circ$. The measurements reveal two prominent peaks related to the emission of a specific number of electrons (horizontal axis): left peak, events with *no* emission of electron (width given by noise spectrum of SBD); second peak, events with emission of *one* electron. A weak peak at the right stems from events for two electrons emitted. The vertical axis represents from top to bottom increasing flight times (energy loss). The spectra provide complete information on the inelastic processes in terms of a variant of translation energy spectroscopy, well established in gas-phase collisions.²⁰

In Fig. 2, we display projections of the spectra from Fig. 1 onto the TOF axis separated with respect to specific num-

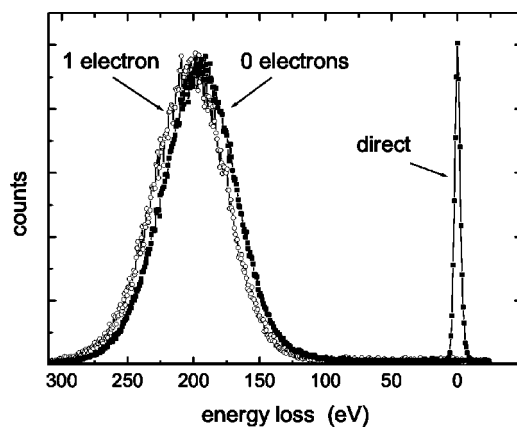


FIG. 2. Energy loss spectra for emission of no (full circles) and one (open circles) electron from data shown in Fig. 1.

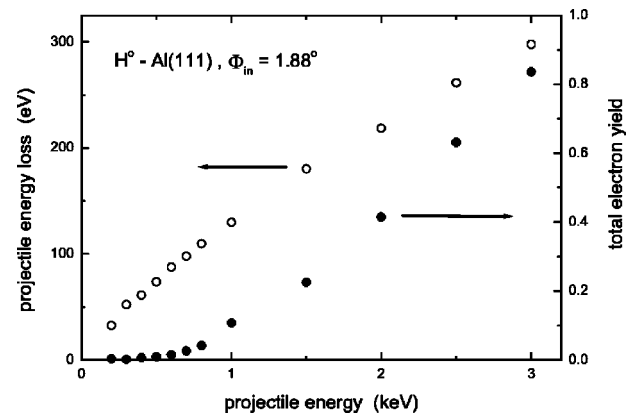


FIG. 3. Total electrons yields (full circles) and mean energy loss (open circles) as a function of projectile energy for scattering of H^+ atoms from Al(111) under $\Phi_{in} = 1.88^\circ$.

ber of emitted electrons: no electron (full circles) and one electron (open circles). Note that in comparison to a recent work using wide-band-gap insulator targets, no discrete structures in the TOF spectra^{16,17,19} can be identified for the metal target. Here the projected TOF spectra integrated over the pulse heights related to the emission of no and one electron show a mutual energy shift of about 8 eV. The additional energy loss associated with the emission of an electron is ascribed to the transfer of projectile energy to one conduction electron in order to overcome the surface potential and to reach vacuum (see also below). This energy shift is much smaller than the mean projectile energy loss of about 200 eV for this case. The total electron yield (derived from integration of spectra for specific SBD pulse heights) amounts to $\gamma \approx 0.2$, so that electron emission requires a negligible fraction of the dissipated projectile energy here (about 1% of total projectile energy loss).

The different behavior of projectile energy loss and total electron yield is demonstrated in Fig. 3 from plots as a function of projectile energy for scattering of H^+ atoms from Al(111). A striking feature in comparing the two datasets is the indication of a kinetic threshold for electron yields which is absent for projectile energy loss. An analysis on projectile stopping showing a weak dependence on angle of incidence is consistent with the established relation of the electronic stopping power $-dE/dx \sim v$. In response theory, the dominant mechanism for projectile energy loss is described by scattering of conduction electrons in the screened potential of the projectile.²¹ The excitation of Fermi electrons is expected to have a very low kinematic threshold. Indeed, a finite ΔE is found in our experiments down to projectile energies, where total electron yields γ have already become close to zero.

We performed detailed studies on the threshold behavior of electron emission for He^+ projectiles that are better to handle with our setup at lower energies. The technique used here has been demonstrated with insulator targets to obtain reliable γ as low as about 10^{-5} .^{17,19} For scattering from metal targets, the energy distributions for scattered atoms are broader and have smaller relative shifts (cf. Fig. 2) between specific electron numbers than observed with insulator tar-

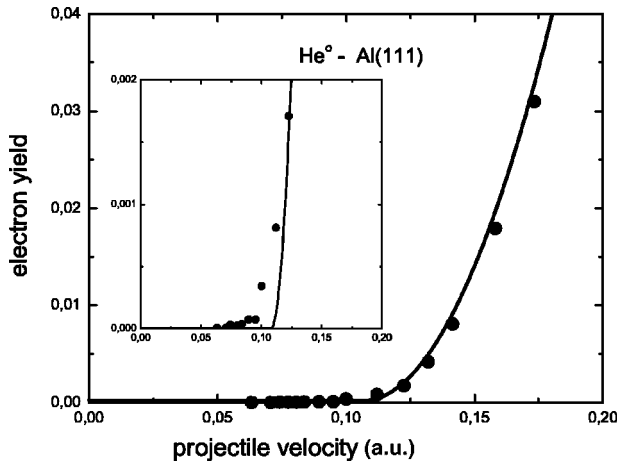


FIG. 4. Total electron yields as function of projectile energy for He° (full circles) atoms scattered from Al(111) under $\Phi_{in}=1.88^\circ$. Solid curve: model calculations as outlined in text. Inset: vertical scale enlarged by factor of 20.

gets. As a consequence, it is more difficult at low γ to correct for cross talk from the dominant TOF spectrum coincident with emission of no electron to the TOF spectrum for emission of one electron. Therefore, the absolute uncertainties in the determination of very low total electron yields are estimated here to typically about 10^{-5} . To our knowledge, this level of sensitivity has not been achieved in experiments so far.

In Fig. 4, we display total electron yields for impact of He° atoms (full circles) as a function of projectile velocity which show within the limits of the experiment evidence for a kinetic threshold. The solid curve in Fig. 4 represents the best fit to a simple classical model of electron emission for a free-electron metal, where emission near threshold is assumed to result from a transfer of energy from projectiles to electrons in binary head-on collisions. Due to the vastly different masses of projectile (M) with initial momentum $M\vec{v} = M(v_{\parallel}, v_z) \approx M(v, 0)$ and electron (m_e) with $\vec{k} = (k_{\parallel}, k_z)$, the final electron momentum is $\vec{k}' = (-k_{\parallel}, k_z) + \vec{q}$ with $\vec{q} = 2m_e(v, 0)$. The density of occupied electronic states in a free-electron metal is represented in momentum space by the ‘‘Fermi sphere’’ of radius k_F (Fermi momentum).

Electrons with initial states within the Fermi sphere can be ejected to vacuum, when the condition $\vec{k}'^2/2m_e = (\vec{k}_F + \vec{q})^2/2m_e \geq E_F + W$ holds, resulting in a threshold for momentum transfer to vacuum $q_{th} = 2m_e v_{th}$, with v_{th} given by Eq. (1). For maximum-energy transfer, electrons are excited parallel to the direction of incident projectiles (elastic-scattering events ensure emission to vacuum). The phase space available for electron emission is given by occupied metal states that fulfill the condition $|\vec{k}'| \geq k_F + q_{th}$. This condition can be visualized in momentum space by a Fermi sphere shifted with respect to its origin by momentum \vec{q} where the Fermi-sphere volume outside of a sphere of radius $k_F + q_{th}$ represents the density of states with vacuum energies. As outlined in detail in a forthcoming paper, one can derive from simple geometrical arguments relative total electron yields near threshold

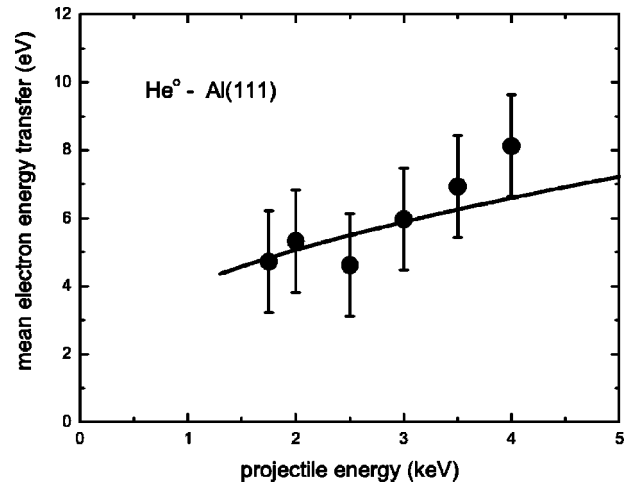


FIG. 5. Mean electron energy transfer as a function of projectile energy for He° atoms scattered from Al(111) under $\Phi_{in}=1.88^\circ$. Solid curve: model calculations (details see text).

$$\gamma \sim 4\pi m_e^3 (v_F + v_F^2/v_{th})(v - v_{th})^2. \quad (2)$$

The solid curve in Fig. 4 represents the best fit of the data by Eq. (2) with a proportionality factor and v_{th} as parameters. For an Al(111) surface with work function $W = 4.29 \text{ eV} = 0.157 \text{ a.u.}$ (Ref. 22) and Fermi energy $E_F = 10.6 \text{ eV} = 0.389 \text{ a.u.}$,²³ we derive from Eq. (1) $v_{th} = 0.082 \text{ a.u.}$ and a projectile energy $E_{th} = 167 \text{ eV/amu}$. Such a threshold is consistent with the data shown in the inset, however, from our fit we obtain $v_{th} = 0.112 \text{ a.u.}$ This result can be explained by the decay of electron density n_e in front of the surface. For our scattering conditions, the distance of closest approach amounts to about 3 a.u.,¹⁵ where the density of conduction electrons and therewith v_F are considerably smaller than the respective bulk properties. Our value for v_{th} corresponds to a reduction of v_F to 65%, in good agreement with calculations of n_e for an Al surface showing about 25% of the bulk density at 3 a.u. ($v_F \sim n_e^{1/3}$).²⁴ The small fraction of projectiles showing a lower v_{th} (cf. inset of Fig. 4) is attributed to trajectories affected by surface defects (steps, etc.), where electron densities are close to bulk values.

From the difference of the mean projectile energy losses related to emission of one and no electron (cf. Fig. 2), we deduce mean energies transferred to electrons ejected into vacuum as plotted for He° projectiles in Fig. 5. Note that these energies are close to the target work function of 4.29 eV so that electrons emitted to vacuum possess energies of typically eV only.

The solid curve in Fig. 5 represents calculations using our binary encounter model, where, for a given momentum q , phase space for electron emission with kinetic energy $E_e = m_e v_e^2/2$ in vacuum results from the overlap of the surface of a sphere of radius $(k_F + q_{th} + m_e v_e)$ with the volume of the shifted Fermi sphere (see above). From this overlap as function of E_e we compute mean electron energies as plotted in Fig. 5 which are in quantitative agreement with experiment.

In conclusion, for kinetic electron emission of fast H° and He° atoms during grazing impact on Al(111) we find evidence for a threshold behavior. The threshold behavior can be described by a purely classical model of energy transfer from projectiles to electrons in binary encounters in a free-electron gas. As a specific feature of grazing surface scattering we find that the threshold is related in a consistent manner to the reduced electron density in the selvage of the metal surface. The clear-cut different energy dependence of the projectile energy loss in comparison to the electron emission yield may be understood by the small excitation energies for

conduction electrons which are negligible within metals, whereas for emission electrons have to overcome the surface potential barrier (work function) for which a minimum-energy transfer from the projectile energy is needed. In this respect, we hope that our work will stimulate first-principles treatments on this fundamental problem of atomic collision with solids.

We acknowledge helpful discussions with Professor A. Arnau and Dr. I. Juaristi (San Sebastian). Work was supported by DFG (Grant No. Wi 1336) and by Austrian Fonds FWF (Grant No. P14337-PHY).

*Author to whom correspondence should be addressed. Electronic address: winter@physik.hu-berlin.de

¹J.J. Thomson, *Philos. Mag.* **23**, 449 (1912).

²L.H. Thomas, *Proc. Cambridge Philos. Soc.* **23**, 713 (1927).

³M. Gryzinsky, *Phys. Rev.* **115**, 373 (1959).

⁴A.E. Kingston, *Proc. Phys. Soc. London* **87**, 193 (1966).

⁵W. Lotz, *Z. Phys.* **206**, 205 (1967).

⁶T.D. Märk, in *Electron-Molecule Interactions and Their Applications*, edited by L.G. Christophorou (Academic Press, New York, 1984), Vol. 1, p. 251.

⁷D. Hasselkamp, *Springer Tracts Mod. Phys.* **123**, 1 (1992).

⁸R.A. Baragiola, in *Low Energy Ion-Surface Interactions*, edited by J.W. Rabalais (Wiley, New York, 1994), p. 187.

⁹A. Zangwill, *Physics at Surfaces*, (Cambridge University Press, Cambridge, England, 1988).

¹⁰J. Lörincik, Z. Sroubek, H. Eder, F. Aumayr, and HP. Winter, *Phys. Rev. B* **62**, 16 116 (2000).

¹¹J.W. Rabalais, H. Bu, and C.D. Roux, *Phys. Rev. Lett.* **69**, 1391 (1992).

¹²G. Lakits, F. Aumayr, and HP. Winter, *Rev. Sci. Instrum.* **60**, 3151 (1989).

¹³M.W. Thompson, in *Channeling*, edited by D.V. Morgan (Wiley, London, 1973), p. 1.

¹⁴D.S. Gemmell, *Rev. Mod. Phys.* **46**, 129 (1974).

¹⁵H. Winter, *Phys. Rep.* **367**, 387 (2002).

¹⁶P. Roncin, J. Vilette, J.P. Atanas, and H. Khemliche, *Phys. Rev. Lett.* **83**, 864 (1999).

¹⁷A. Mertens, S. Lederer, K. Maass, H. Winter, J. Stöckl, HP. Winter, and F. Aumayr, *Phys. Rev. B* **65**, 132410 (2002).

¹⁸C. Lemell, J. Stöckl, HP. Winter, and F. Aumayr, *Rev. Sci. Instrum.* **70**, 1653 (1999).

¹⁹A. Mertens, K. Maass, S. Lederer, H. Winter, H. Eder, J. Stöckl, HP. Winter, F. Aumayr, J. Vieffhaus, and U. Becker, *Nucl. Instrum. Methods Phys. Res. B* **182**, 23 (2001).

²⁰H.B. Gilbody, *Adv. At., Mol., Opt. Phys.* **32**, 149 (1994).

²¹P.M. Echenique, R.M. Nieminen, and R.H. Ritchie, *Solid State Commun.* **37**, 779 (1981).

²²A.G. Borisov, D. TeilletBilly, J.P. Gauyacq, H. Winter, and G. Dierkes, *Phys. Rev. B* **54**, 17 166 (1996).

²³H.J. Levinson, F. Greuter, and E.W. Plummer, *Phys. Rev. B* **27**, 727 (1983).

²⁴K. Bohnen (unpublished).